African Journal of Environment and Natural Science Research
ISSN: 2689-9434
Volume 6, Issue 3, 2023 (pp. 67-87)
www.abjournals.org

INVESTIGATING THE SUSCEPTIBILITY OF TUNNEL EROSION IN SOUTHERN NIGERIA USING INTEGRATED GEOPHYSICAL METHODS

Chibuogwu I.U.[1*] and Ugwu G.Z.[2]

[1]Nnamdi Azikiwe University Awka, Anambra, Nigeria.

*Corresponding Email: iu.chibuogwu@unizik.edu.ng

[2]Enugu State University of Science and Technology Agbani, Enugu

Email: ugwugz@yahoo.com

Cite this article:

Chibuogwu I.U., Ugwu G.Z. (2023), Investigating the Susceptibility of Tunnel Erosion in Southern Nigeria using Integrated Geophysical Methods. African Journal of Environment and Natural Science Research 6(3), 67-87. DOI: 10.52589/AJENSR-DDBGL2HW

Manuscript History

Received: 12 July 2023

Accepted: 3 Sept 2023

Published: 26 Oct 2023

ABSTRACT: *There has been a growing incidence of soil subsidence in various regions of Anambra State, located in southern Nigeria. These subsidence events primarily stem from the formation of natural tunnels or soil pipes within the subsurface. To delve deeper into this issue, the present study employed two geophysical techniques, namely the Very Low Frequency Electromagnetic (VLF-EM) method and the Electric Resistivity Method utilizing the Dipole-Dipole array. These methods were utilized to investigate the characteristics and spatial distribution of soil pipes at two specific sites: Awka Site 1 and Awka Site 2, both situated within Anambra State, Nigeria. On each profile of the VLF-EM, the inphase and outphase were collected using the Abem Wadi Meter after a confirmed connection to the external satellite, while nine dipole-dipole profiles were carried on the same location. The data analysis from the VLF-EM survey reveals that a significant portion (80%) of the low conducting zones observed in the pseudosection originates from the top of the profile, indicating a downward trend in the formation of soil piping. The VLF-EM result also inferred that the subsurface voids in the study areas extend vertically downward up to 10 meters, with an average horizontal extension exceeding 0.5 meters. This highlights the extensive spatial reach of the subsurface voids and emphasizes their potential impact on the surrounding environment. The dipole-dipole survey conducted in the study area identified six distinct structures, with the eroded formation being particularly noteworthy. This structure, characterized by resistivity ranging from 1200–30000 Ωm, plays a significant role in creating favorable conditions for soil piping. Furthermore, the presence of strong dispersive soils increases the likelihood of soil piping occurrences within this structure.*
KEYWORDS: *Soil Piping; Tunnel Erosion; Erosion, Soil Subsidence, VLF-EM, Dipole-Dipole, Resistivity, Conductivity, Dispersion.*

Keywords: Soil Piping, Tunnel Erosion, Erosion, Soil Subsidence, VLF-EM, Dipole-Dipole, Resistivity, Conductivity, Dispersion.

Article DOI: 10.52589/AJENSR-DDBGL2HW
DOI URL: https://doi.org/10.52589/AJENSR-DDBGL2HW

African Journal of Environment and Natural Science Research
ISSN: 2689-9434
Volume 6, Issue 3, 2023 (pp. 67-87)

www.abjournals.org

INTRODUCTION

Erosion is a geological process whereby earth materials are gradually moved and transported by natural forces like wind and flowing water (Dodds, 2003; Wilson et al., 2008; Zhu et al., 2002). Different types of erosion exist; the most common are the gullies, sheets, rills, and tunnels. Tunnel erosion, also known as soil piping, occurs when the soil beneath the earth's surface is worn out, resulting in the formation of underground channels (Bernatek-Jakiel & Kondracka, 2016; Bernatek-Jakiel & Poesen, 2018; Bernatek-Jakiel & Wrońska-Wałach, 2018; García-Ruiz et al., 1997). Initially, soil piping begins as small pores within the subsurface before enlarging to form channels where soil and other materials are transported. With time, the roof where these particles are transported may become weak and collapse, leading to both surface and subsurface erosion - land subsidence (Graham & Lin, 2012; Jones et al., 1997; Parker et al., 1990; Sidle et al., 1995; Zhang & Wilson, 2013; Zhu et al., 2002).

Soil piping is most common in areas with high seasonal rainfall variations, for example, in lateritic terrains or tropical rain forests - making Anambra State an ideal environment for its occurrence (Atallah et al., 2015; Castañeda et al., 2017; Patti et al., 2021; Vannoppen et al., 2017). Gully erosion, landslides, and floods are the common environmental hazards facing Anambra State in the rainy season (Ezenkwen, 2010; Uchegbu, 2004). However, during the last three decades, land subsidence due to the collapse of subsurface roofs and tunnel roofs has largely been reported in various parts of the state (Nich & Okeke-Ogbu, 2017; Uchegbu, 2004). This has reduced the agricultural productivity of the state, and the terrains often become inhospitable (Chibuogwu & Ugwu, 2023a). Development of subsurface tunnels has also altered the hydrogeological process of the area and open wells have often become unsustainable even during high rains (Ezenkwen, 2010; Nich & Okeke-Ogbu, 2017). In many of these events, there have been loss of lives and properties, and people's means of livelihood have been cut short because of imbedded daily activities (Nich & Okeke-Ogbu, 2017). Finances have also been sunk into the control of this soil subsidence in order to reclaim roads, people's properties and valuable farmland by members of the community and the government (Nich & Okeke-Ogbu, 2017; Uchegbu, 2004). The patching up method is commonly employed in tackling soil piping, but little or no progress has been achieved. Hence, the need to abate this unfavorable phenomenon using alternative scientific methods became paramount (Nich & Okeke-Ogbu, 2017; Uchegbu, 2004).

The use of geophysical techniques were considered because they can detect and analyse the extent at which particles beneath the subsurface vary without carrying out a major excavation process that usually requires the need for heavy machineries and often disturb the top soil (Chibuogwu & Ugwu, 2023a, 2023c). This generally incurs a low cost but provides a robust investigation of the environment at large. It is also necessary to carry out a soil and water analysis of the area in order to detect causative features of the soil piping.

Thus, in this study, we aimed to investigate the spatial distribution, pattern, and characteristics of soil pipes in an area known with tunneling erosion in Awka, Anambra State, Nigeria. To achieve this goal, we employed two direct current techniques: Very Low Frequency Electromagnetic (VLF-EM) and Electrical Resistivity Tomography (ERT). These methods were used to gain a better understanding of the complexity and characteristics of the soil-piping network. By utilizing ERT and VES, we were able to achieve a more comprehensive understanding of the subsurface soil conditions in the area. The findings of these investigations

Article DOI: 10.52589/AJENSR-DDBGL2HW
DOI URL: https://doi.org/10.52589/AJENSR-DDBGL2HW

will allow for the identification of anomalous features contributing to soil piping and offer insights into possible strategies for tracking and reducing its effects.

GEOLOGY AND LITHOSTRATIGRAPHY OF STUDY AREA

Figure 1 illustrates the study area, which is located within the Anambra Sedimentary Basin in southeastern Nigeria. The basin encompasses an area of approximately 40,000 km², with its southern boundary aligning with the delta swamps of the Niger Delta Basin. Additionally, the basin stretches northward beyond the Bende Ameki Formation. It is widely believed that the basin was formed concurrently with the folding and upsurge of the Abakaliki-Benue area during the Santonian epoch. The Anambra Basin serves as a primary depositional center for clastic deposits and deltaic sequences, having emerged from the second Lower Benue Trough tectonic activity. Figure 1(a) depicts the geological map of Nigeria, along with the Anambra Basin.

The soils in Anambra State, specifically those identified as coastal plain sands, possess groundwater reservoirs. Unfortunately, these reservoirs contribute significantly to ecological problems in the area. These soils are highly vulnerable to erosion, and the underlying geological rocks and materials are strikingly unstable and poorly consolidated.

Of particular concern are the sandy portions of these geological units, which host large groundwater reservoirs known as aquifers. When these aquifers experience pore water pressures due to overlying structures carrying uncompromising loads, they can become a dangerous threat. Further exacerbating the situation is the ease with which the lateritic and sandy soils are eroded when exposed to storm water runoffs.

Article DOI: 10.52589/AJENSR-DDBGL2HW
DOI URL: https://doi.org/10.52589/AJENSR-DDBGL2HW

African Journal of Environment and Natural Science Research
ISSN: 2689-9434
Volume 6, Issue 3, 2023 (pp. 67-87)
www.abjournals.org

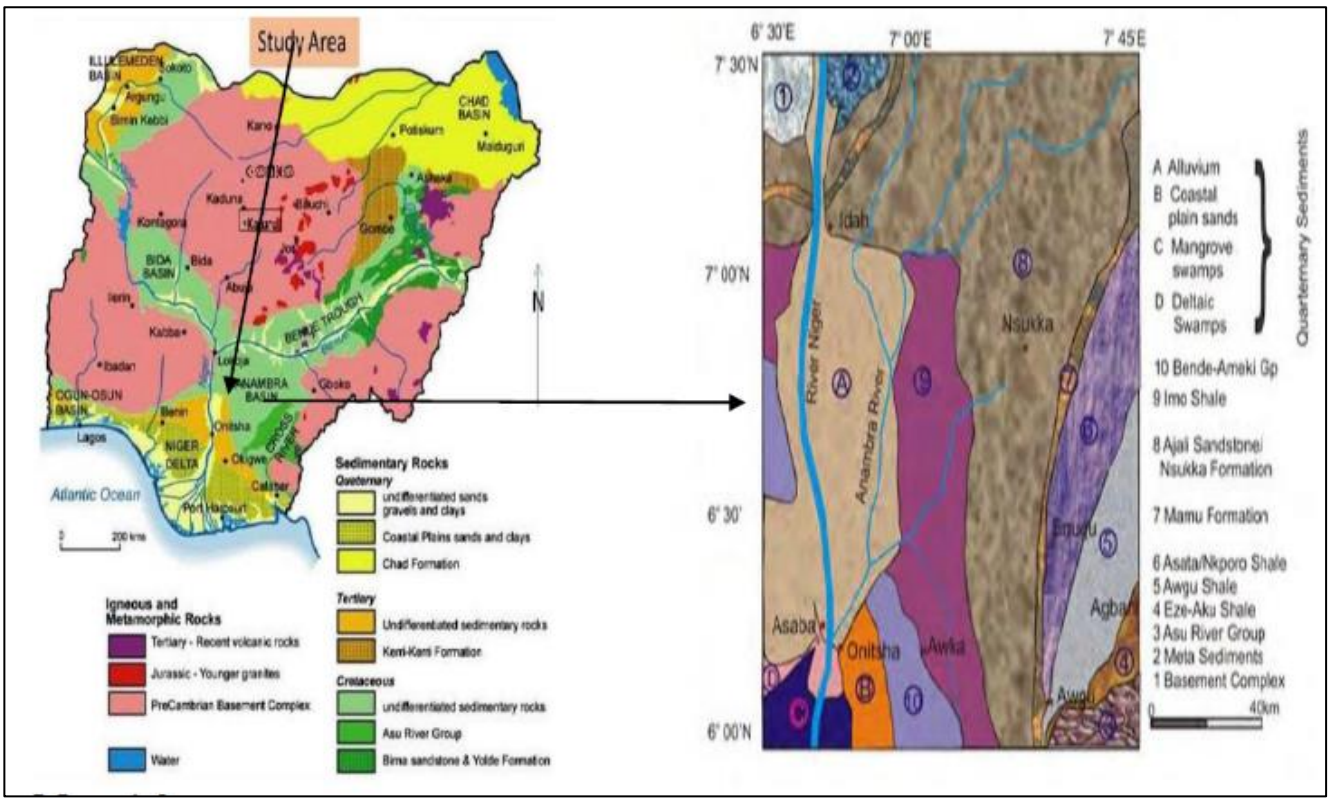

Figure 1: Map of the geological setting of Nigeria and Anambra Basin

STUDY AREA

The focus of this study is centered on Awka, the capital of Anambra State, Nigeria, consisting of two distinct sites (Figure 2) located at coordinates (Lat. 6.2220E and Long. 7.0821E). The first site, Awka Site 1, is situated in close proximity to Paul University in Awka at coordinates (6.22320N and 7.08240E). Here, the 5cm diameter-piping hole has inflicted significant harm, leading to the formation of double sinkholes (soil subsidence) measuring approximately 70cm in diameter (refer to Figure 3). On the other hand, Awka Site 2 is located at the Jerome Udorji Secretariat at coordinates (6.22200N and 7.08190E). This conspicuous piping hole has been present for approximately three years, resulting in several holes with an average diameter of 10cm and a visible sinkhole measuring approximately 300cm in diameter (refer to Figure 4). By minutely examining both sites, we can gain insightful knowledge regarding the characteristics and formation of soil pipes in areas of subsidence.

Article DOI: 10.52589/AJENSR-DDBGL2HW
DOI URL: https://doi.org/10.52589/AJENSR-DDBGL2HW

African Journal of Environment and Natural Science Research
ISSN: 2689-9434
Volume 6, Issue 3, 2023 (pp. 67-87)
www.abjournals.org

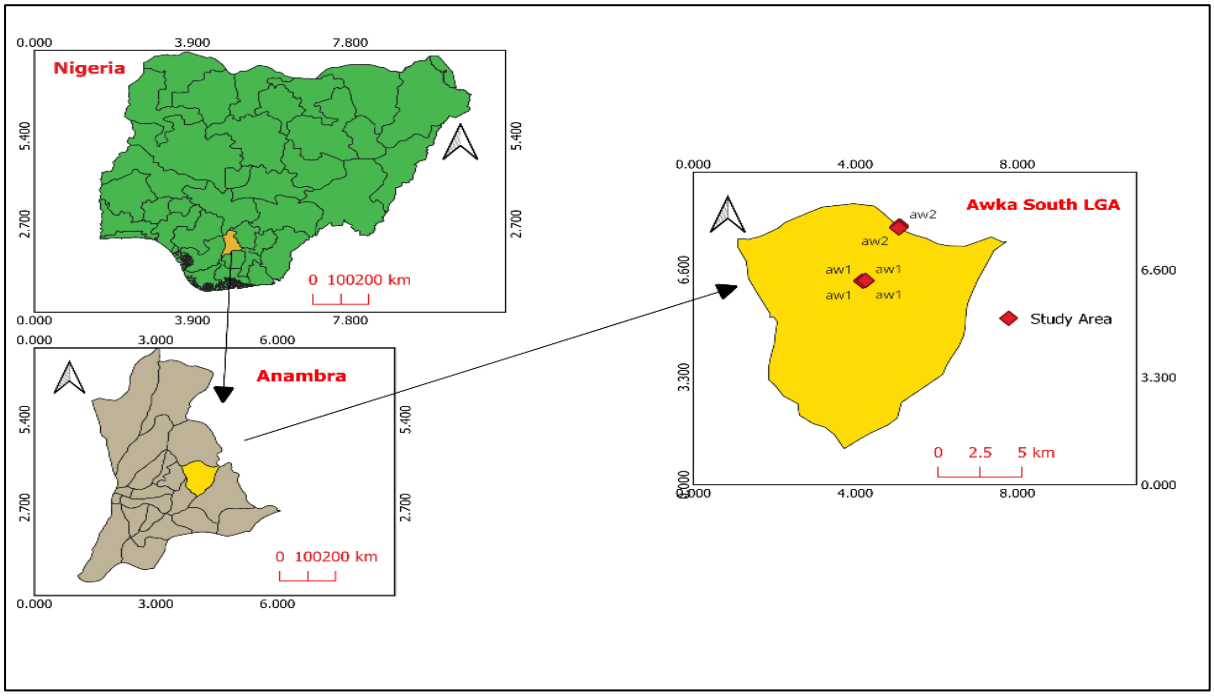

Figure 2: Map showing the surveyed state and LGA

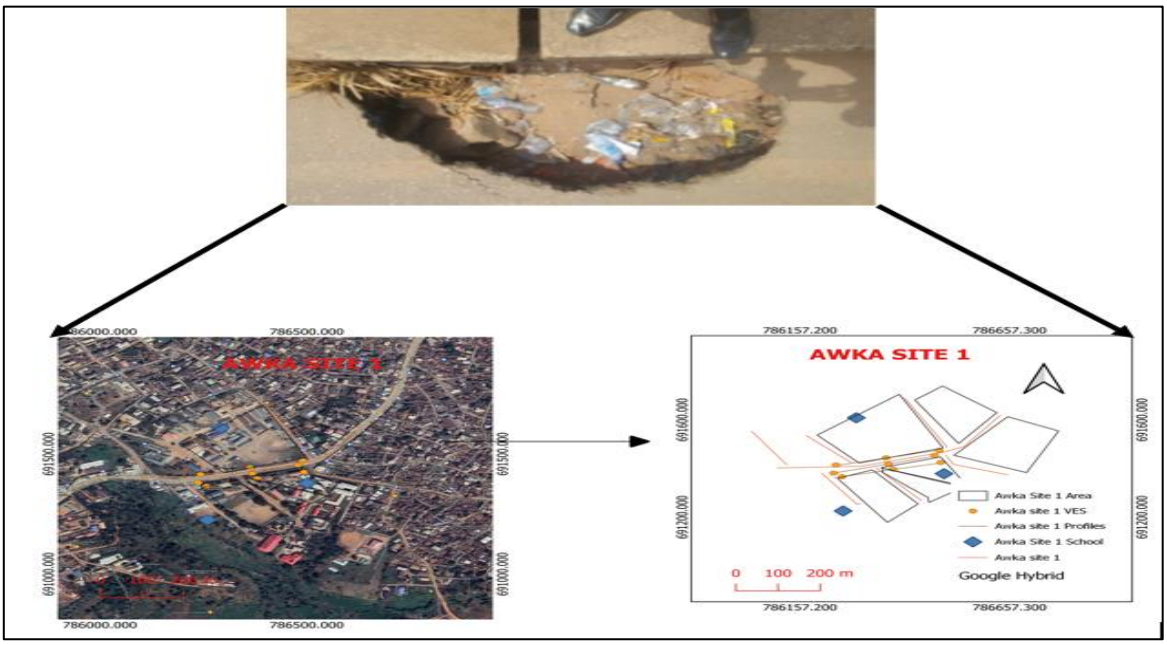

Figure 3: Map of Awka Site 1 showing the subsidence, satellite image and survey points

Article DOI: 10.52589/AJENSR-DDBGL2HW
DOI URL: https://doi.org/10.52589/AJENSR-DDBGL2HW

African Journal of Environment and Natural Science Research
ISSN: 2689-9434
Volume 6, Issue 3, 2023 (pp. 67-87)
www.abjournals.org

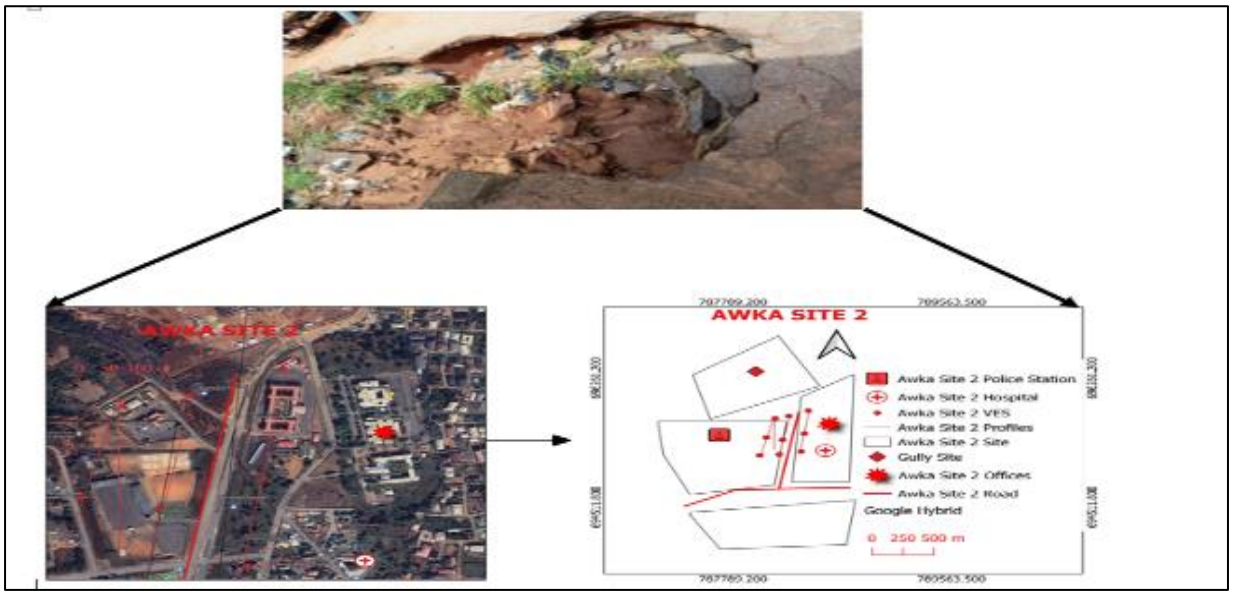

Figure 4: Map of Awka Site 2 showing the subsidence, satellite image and survey point

METHODS

VLF-EM Method

The VLF-EM method is a low-cost and less cumbersome geophysical technique. It primarily uses a primary EM waves from a nearby satellite to induce secondary EM waves in the form of eddy currents to map shallow subsurface structural features (Palacky, 1981).

The VLF meter, ABEM WADI VLF EM, is a battery powered digital indicator that uses a transmitter operating between 15KHz and 25KHz from a powerful radio satellite to generate a very weak time-varying electromagnetic field, the primary field, which can travel very long distances, penetrating the subsurface to induce eddy current, the secondary field, in the buried conductor (Kaikkonen & Sharma, 1998; Palacky et al., 1981).

The ABEM WADI VLF measures the primary field, the secondary field, and the phase lag between the primary and secondary fields. When analysed, this information can be used to detect the presence of a conductor or conductive zone in the ground. For example, a phase lag of the secondary EM field relative to the primary EM field of about half a period (180^0) indicates a conductive ground. A ground with a high resistivity (a poor conductor) will cause the secondary EM field to lag the primary field by a period of 90^0 (Monteiro Santos et al., 2006). For the VLF-EM data analyses, the RAMAG and KHFfilt software (Onwuegbuchulam et al., 2013) were used to find the characteristics of the cross-sectional depth wise of a single profile and filtering, respectively.

Karous-Hjelt filters are an example of linear filters that process the real and imaginary components of the magnetic field, while Fraser filters operate on the tilt angle (Fraser, 1996). The ellipticity and tilt angle of the polarization ellipse are used in the calculation of the real and imaginary responses. The tilt angle (∅) is the angle of the major axis of the ellipse, while

Article DOI: 10.52589/AJENSR-DDBGL2HW
DOI URL: https://doi.org/10.52589/AJENSR-DDBGL2HW

African Journal of Environment and Natural Science Research
ISSN: 2689-9434
Volume 6, Issue 3, 2023 (pp. 67-87)

www.abjournals.org

the ellipticity (e) (Fraser, 1996; Karous & Hjelt, 1983) is the ratio of the minor axis to the major axis, as described by the following equations below (Osinowo & Olayinka, 2012).

$$Tan(2\theta) = \pm \frac{2\left(\frac{H_z}{H_x}\right) Cos\Delta\emptyset}{\left(\frac{H_z}{H_x}\right)^2} \quad (1)$$

$$e = \frac{H_z H_x cos\Delta\emptyset}{{H_i}^2} \quad (1b)$$

where $H_z$and H_x are the amplitude of the phase difference,$\Delta\emptyset = \emptyset_z - \emptyset_x$, and in which $\emptyset_z$is the phase of *Hz* and $\emptyset_x$is the phase of *Hx* and . $H_i = \left|H_z e^{i\Delta\emptyset} sin\theta + H_x Cos\theta\right|$ (2)

From the ellipticity and tilt angle, the real and imaginary responses for a conductor can be calculated from the following equations (Karous & Hjelt, 1983; Ogilvy & Lee, 1991):

$$Real = 100Tan\theta \quad (3)$$

$$Real\% = 100\theta(\theta - inRadian) \quad (4)$$

$$Imaginary = 100e \quad (5)$$

The tangent of the tilt angle is a good approximation of the ratio of the real component of the vertical secondary magnetic field to the horizontal primary magnetic field. The ellipticity is a good approximation of the ratio of the quadrature component of the vertical secondary magnetic field to the horizontal primary field (Monteiro Santos et al., 2006). These quantities are called the real (= tan a × 100 %) and imaginary (= e × 100 %) anomalies, respectively, and they are normally expressed as percentages.

Only the inphase and outphase components are recorded by the ABEM WADI VLF. The ratio of the real component to the imaginary component determines the degree of conductivity (Osinowo & Olayinka, 2012).

Four profiles with transverse lengths of 100 m and 5 m spacing were surveyed (Figures 3 and 4). On each profile, the inphase and outphase were collected on the interface of the Abem Wadi Meter after a confirmed connection to the external satellite. The geographical coordinates of the particular point at which the reading was collected were recorded. Each profile was oriented in a NW-SE direction to follow the stress formation of the study area. This was done to reduce complications due to anisotropic effects associated with the study area.

Dipole-Dipole Method

The measurement of soil pipes and their spatial distribution for this study utilized the dipole-dipole electrode configuration due to its superior horizontal resolution and greater coverage depth in subsurface spaces (Neyamadpour et al., 2010). This particular configuration consists of two pairs of electrodes: a current electrode (transmitter) and a potential electrode (receiver). A dipole is formed by setting two electrodes closely together at one end, and convention

Article DOI: 10.52589/AJENSR-DDBGL2HW
DOI URL: https://doi.org/10.52589/AJENSR-DDBGL2HW

dictates that the distance between the current and potential electrodes is maintained at an equal distance (spacing = a) with each distance being an integer multiple of "a" (J. O. Coker et al., 2020; Li & Rao, 2019). By utilizing this setup, the researchers were able to accurately measure the nature and spatial distribution of soil pipes with high precision and accuracy.

The resistivity survey for this study used a PASI resistivimeter with 24 steel electrodes spaced at 5 meters to achieve a profile length of 100 meters or more, depending on available space. To minimize errors in the survey, all electrodes underwent a constant resistance test at regular intervals prior to the survey, with a maximum desired limit for ground resistance (Rg) set at 10KΩ. Any electrode with an Rg value above this limit was deemed to have poor contact with the ground and was subsequently adjusted by measures such as hammering or applying saline solution, after which the PASI resistivimeter was activated for the actual survey.

The PASI resistivimeter was utilized for the purpose of measuring and collecting resistivity data. The gathered information was then analyzed using DEPROWIN software, which allowed for the development of 2D electrical imaging pseudosections constructed from the measured physical parameters. The program was specifically designed to facilitate inversion of extensive data ranging from 200 to 21000, by utilizing a system consisting of numerous electrodes spanning from 20 to 16000. The pseudosections are divided into rectangular blocks, which are then represented through the optimization of field measurements. This optimization technique works to minimize the difference between the calculated and measured apparent resistivity values by adjusting the model resistivity of the block. This difference is then expressed as the RMS (Root Mean Square) error, as outlined by Carrazza et al. (2016), Loke and Barker (1996).

RESULTS

Figures 5a–5h illustrate the outcome of the VLF-EM geophysical survey, which utilized both Fraser filtering for the current density data response and pseudo-sections of the Karous-Hjelt filtering to visualize the current density data against subsurface depth. The purpose of this survey was to investigate the distribution of soil pipes in the subsurface.

Profiles 1 and 2 were carried out at Awka Site I; Profile 1 was done directly on top of a known soil pipe, while Profile 2 was done 2 km from profile 1 where there is no evidence of soil pipe, sinkhole, or gully erosion. Similarly, Profiles 3 and 4 were projected just as the former profiles, with profile 4 being 1.7 km from Profile 3.

All profiles in this section run from NW to SE, with each measurement station (a transverse of 100m) separated by 5 meters of spacing, except for Profile 4, which had a different orientation due to space restrictions. The pseudosection for the Karous-Hjelt filtering revealed an uneven distribution of conductivities in the subsurface. Different shades of blue were used to represent the various conductivity zones and distinguish distinctive zones in the subsurface. The light blue color represents the intermediate conductivity of the clay zone, while the sandy zone is represented by the not-too-light blue color, indicating low conductivity. The dark blue color represents eroded structures, such as fractured or anomalous zones resulting from very low conductivity.

Article DOI: 10.52589/AJENSR-DDBGL2HW
DOI URL: https://doi.org/10.52589/AJENSR-DDBGL2HW

African Journal of Environment and Natural Science Research
ISSN: 2689-9434
Volume 6, Issue 3, 2023 (pp. 67-87)
www.abjournals.org

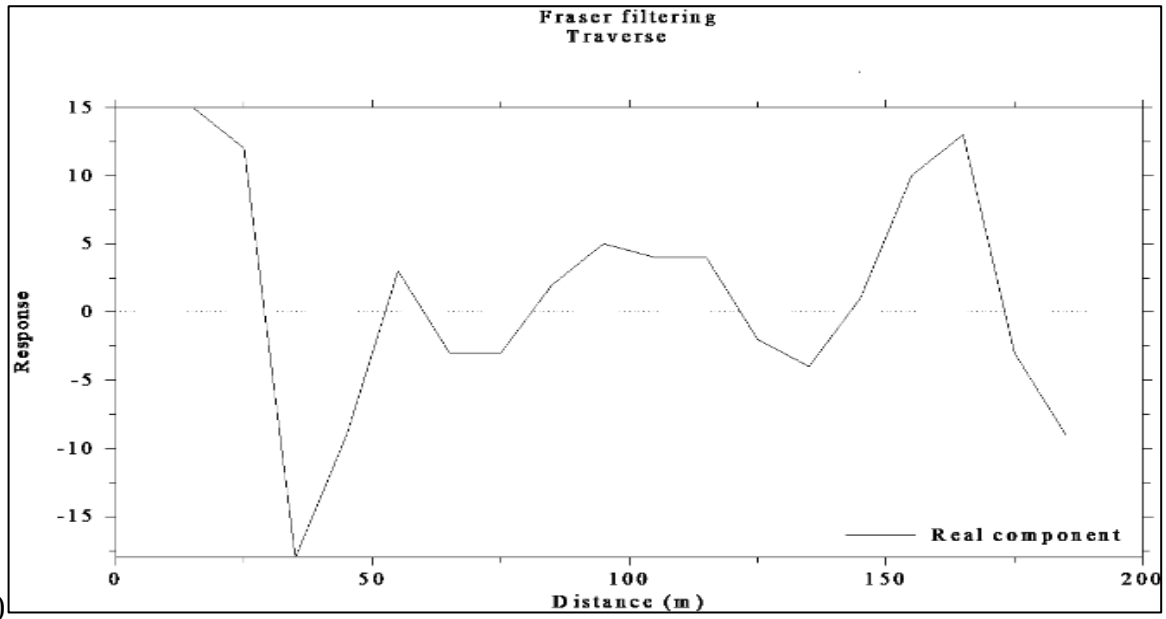

(a)

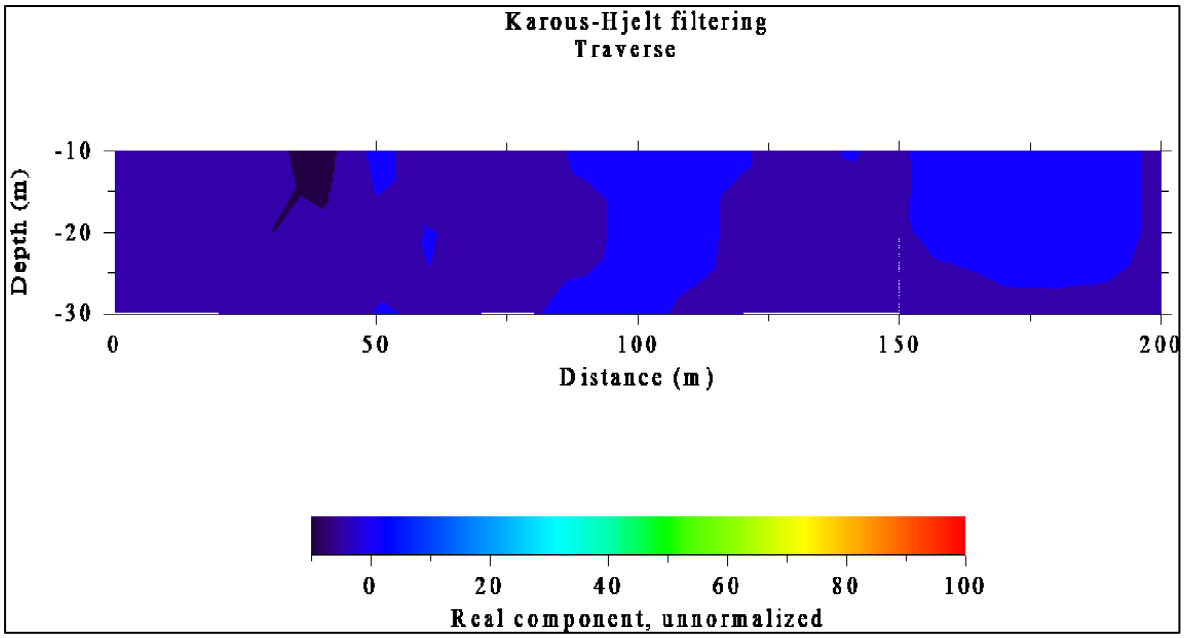

(b)

Article DOI: 10.52589/AJENSR-DDBGL2HW
DOI URL: https://doi.org/10.52589/AJENSR-DDBGL2HW

African Journal of Environment and Natural Science Research
ISSN: 2689-9434
Volume 6, Issue 3, 2023 (pp. 67-87)
www.abjournals.org

(c)

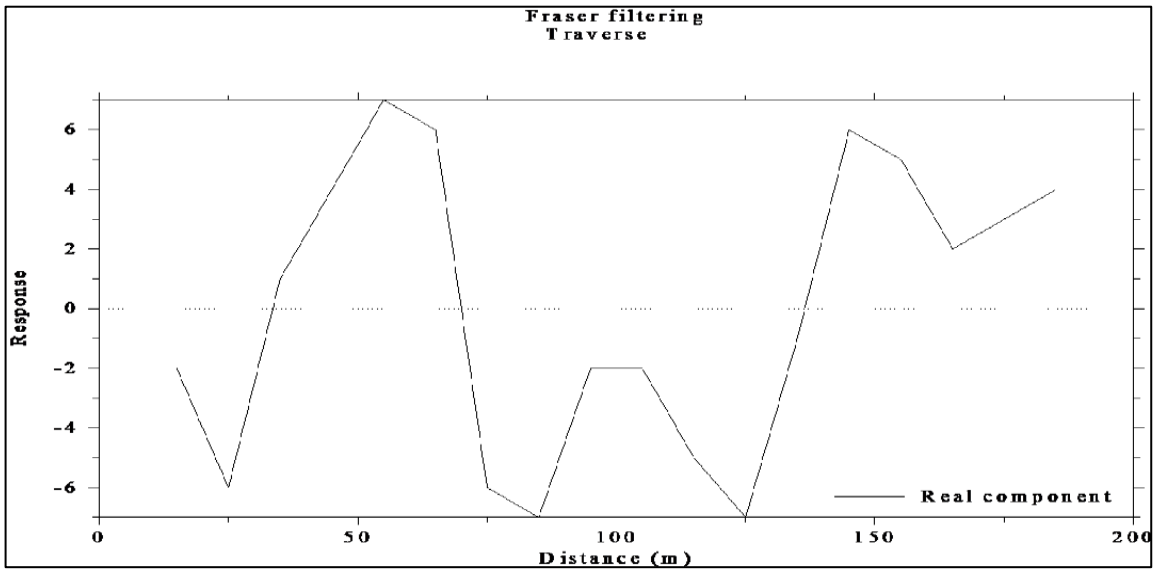

(d)

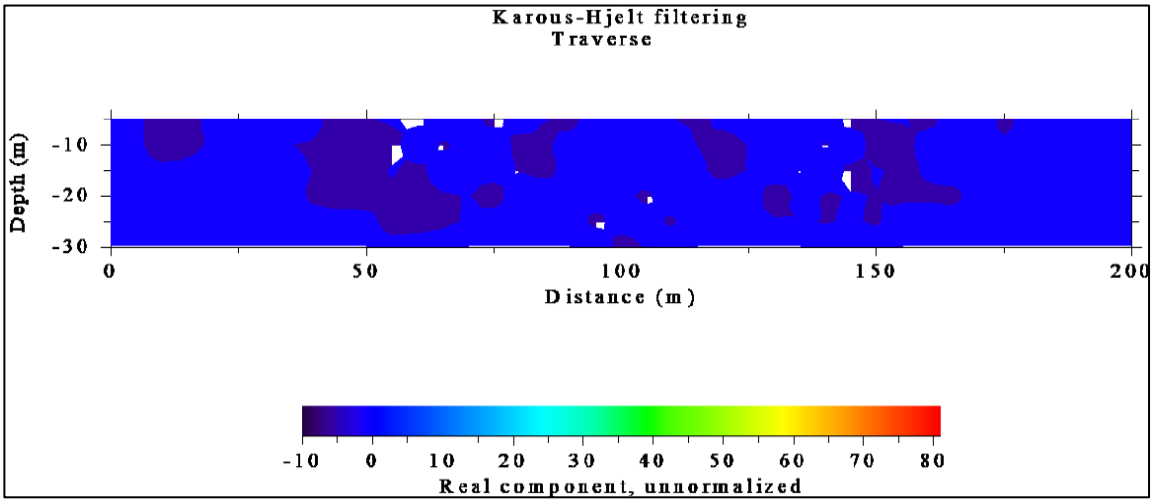

Figures 5a–5d: A graph of Frazer filtering (a and c) and Pseudosection of Karous-Hjelt filtering (b and d) for Awka Site 1

Article DOI: 10.52589/AJENSR-DDBGL2HW
DOI URL: https://doi.org/10.52589/AJENSR-DDBGL2HW

African Journal of Environment and Natural Science Research
ISSN: 2689-9434
Volume 6, Issue 3, 2023 (pp. 67-87)
www.abjournals.org

(e)

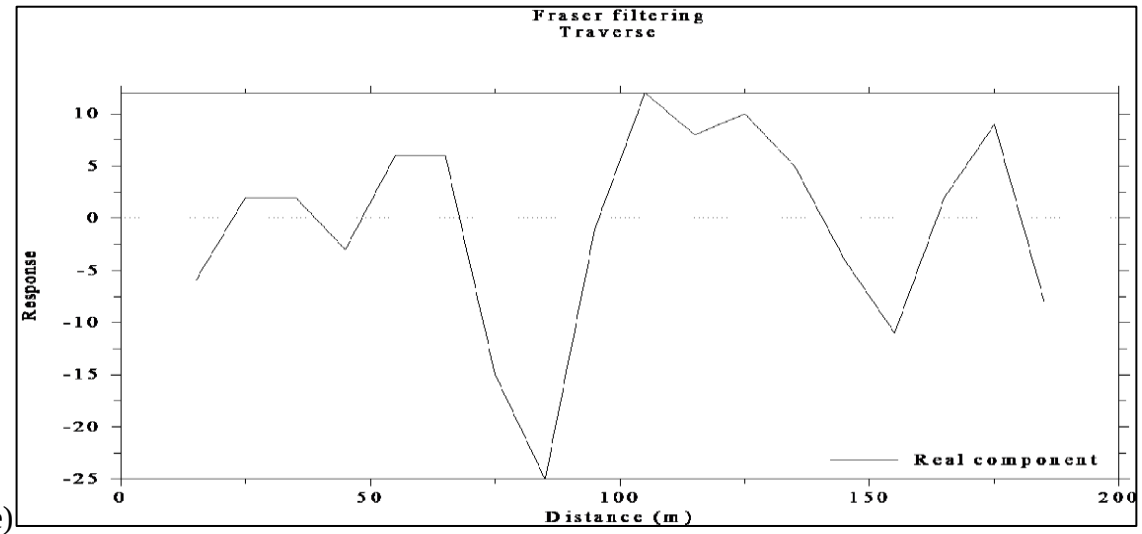

(f)

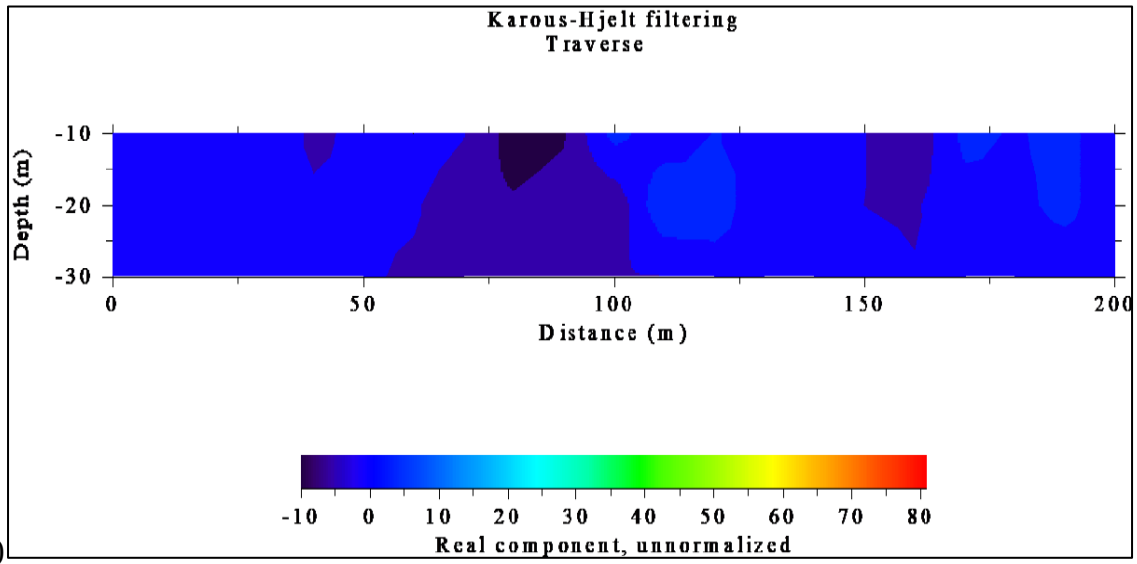

Article DOI: 10.52589/AJENSR-DDBGL2HW
DOI URL: https://doi.org/10.52589/AJENSR-DDBGL2HW

African Journal of Environment and Natural Science Research
ISSN: 2689-9434
Volume 6, Issue 3, 2023 (pp. 67-87)
www.abjournals.org

(g)

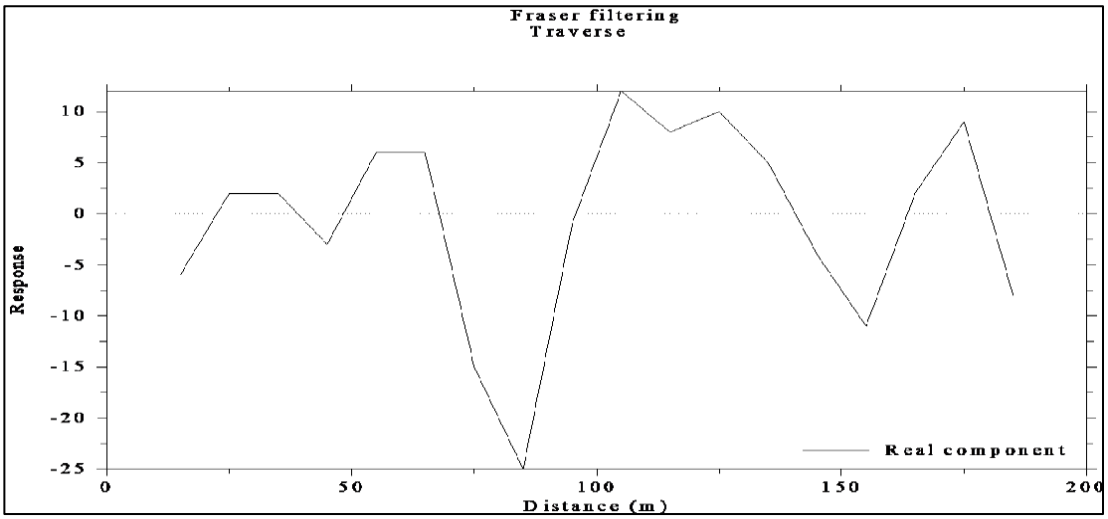

(h)

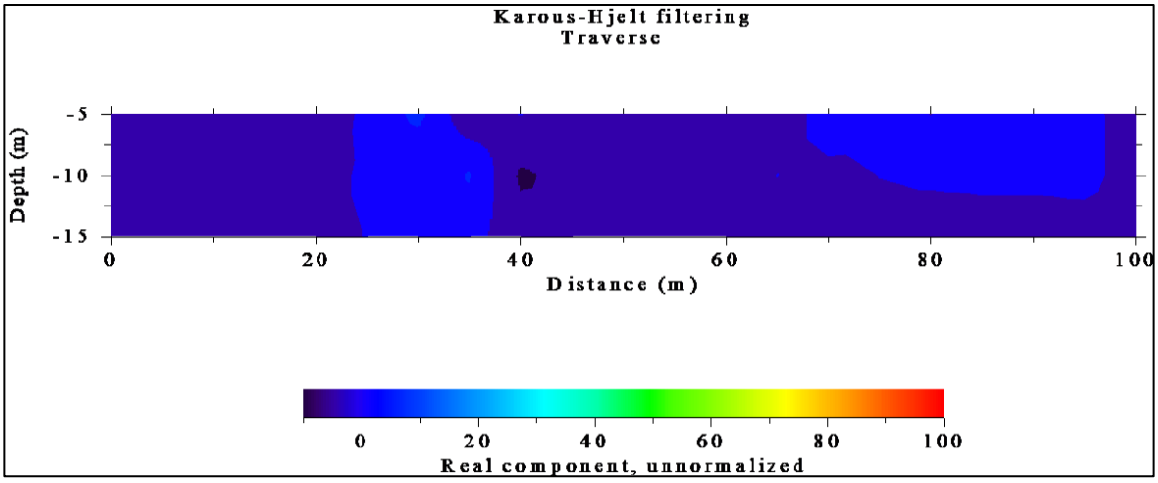

Figures 5e–5h: A graph of Frazer filtering (e and g) and Pseudosection of Karous-Hjelt filtering (f and h) for Awka Site 2

For the Fraser filtering in Figure 5, areas on the graph with a maximum negative anomaly amplitude are considered zones in the subsurface with layers of shallow overburden (eroded) and are likely to reveal major fractures, which in this case may contain air. The areas in Profile 1 (Figure 5a) that could be observed to have maximum negative anomaly amplitude are at response marks 15 and 30, at a profile length of 35 m and 170 m, respectively. For Profile 2 (Figure 5c), these maximum negative amplitudes are observed at response marks 6 and 7 under profile lengths 25 and 124, respectively. At a response mark of 25 under profile length 90m, for Profile 3 (Figure 5e). In Profile 4 (Figure 5g) has two specific areas for maximum negative

Article DOI: 10.52589/AJENSR-DDBGL2HW
DOI URL: https://doi.org/10.52589/AJENSR-DDBGL2HW

anomaly amplitudes located at a response mark of 25 and 10 between a profile length of 80m and 150m respectively.

For Karous-Hjelt filtering, the conductivity of the subsurface ranges from -10 to 100 Mhos. The areas considered to have low conductivity (-10 to 0.5 Mhos) that may favour the formation of soil piping are within profile lengths of 30 m to 40 m in Profile 1, and the depth of this layer is approximately 10m (Figure 5b). For Profile 3 (Figure 5d), it could be observed to have penetrated a depth of 6m in between profile lengths of 60 m and 65 m. There is no evidence of this low conductive zone in Profile 2 (Figure 5f), while a brief dot is observed in Profile 4 (Figure 5h).

Result for Dipole-Dipole

In this comparative study, the 2D resistivity imaging data collected via the dipole-dipole array were subjected to a robust inversion method. The inversion process involved nine iterations; at the completion, the process had converged with an RMS misfit of 7.39%. Six distinct images were then generated through the process, which are outlined in Profile 1 through Profile 6.

Figures 6 and 7 provide an overview of the inversion process carried out on Profile 1 through 3 at Awka Site 1 and on Profile 4 through 6 at Awka Site 2. The orientation of each profile was chosen to match the NW-SE direction of the study area, taking into consideration the strain directions of the subsurface materials and to reduce the anisotropic effect. The first observation made from the inversion output shows that the profiles exhibit anisotropic resistivity distribution, leading to six distinct structures labeled A, B, C, D, P, and bedrock. Structure A, represented by blue colors, refers to the fault or fracture zone with saturated content. Structure B, identified with green color, corresponds to clayey. Sandy clay is represented by the yellow-colored structure C, while structure D, identified by the red color, corresponds to sand. The letter P is used to identify an eroded structure illustrated by purple color, which could potentially be the location for soil pipes.

Profile 1

This profile was placed 3 meters west of a known soil pipe (Figure 6a) and surveyed over a length of 200 meters using an electrode spacing of 5 meters. The maximum depth probed was 25 meters, with resistivity values ranging from 1 to 400 Ωm. The top of the profile reveals a finely stretched structure labelled D with resistivity ~250 Ωm. Within this structure are the zones with the highest resistivity ~ 400 Ωm, labeled P. They come in three different patches. The first patch is located at the northern end of the profile within electrodes 20–30 at a depth of 3 m while the other patches are located at the center of the profile beneath electrodes 65 and 95 respectively and at a depth of 5 m. The low-resistivity zones, labelled A, with an approximate resistivity of 20Ωm are well imaged. They may be considered to be saturated with water. Sandwiching the water-bearing zone is the clay labelled C with resistivity ~180 Ωm.

Profile 2

Profile 2 was laid directly on top of the soil pipe (Figure 6b). A profile length of 100m was surveyed with an electrode spacing of 5 m and a maximum depth of 25 m was probed. The profile is characterized by resistivity ranging from 899–38999 Ωm. The inversion output described similar anisotropic structures like those in Profile 1. At the top of the profile is the zone labeled D, the fine sand with an approximate resistivity of 16000 Ωm. Within this zone

Article DOI: 10.52589/AJENSR-DDBGL2HW
DOI URL: https://doi.org/10.52589/AJENSR-DDBGL2HW

African Journal of Environment and Natural Science Research
ISSN: 2689-9434
Volume 6, Issue 3, 2023 (pp. 67-87)
www.abjournals.org

(D) are patches labeled P, the eroded soils, with very high resistivity ~38999 Ωm, located at the northern and at the center of the profile. At the extreme south of the profile is a squared zone known as the bedrock with resistive that is way beyond 40000 Ωm. Surrounding these high resistivity zones are regions with bright yellow colour, labeled C with resistivity of ~7500 Ωm and just below the region are the clayey soil, labeled B with an approximate resistivity of 3161 Ωm. The zone label A, with resistivity of ~ 900 Ωm, is saturated with water.

Profile 3

Profile 3 (Figure 6c) was laid 3 m east of the soil pipe. A profile length of 100 m was surveyed with an electrode spacing of 5 m. As in the two previous profiles, a maximum depth of 25 m was probed. The profile is characterized by resistivity ranging from 39–1199 Ωm. At the top of the profile is a zone considered to be composed of saturated materials penetrating a depth of 5 m with a very low resistivity of ~40 Ωm. They can be observed in four patches, scattered at different parts of the profile. Surrounding the saturated materials is the clay zone labeled B with resistivity of ~100 Ωm. The thick purple region that covers about 70% of the profile is interpreted as bedrock. In between the bedrock and the clayey zone are two thin regions, labelled C and D, highly stratified with intermediate resistivity, approximately 200 Ωm and 400 Ωm respectively, cutting from one end of the profile to the other.

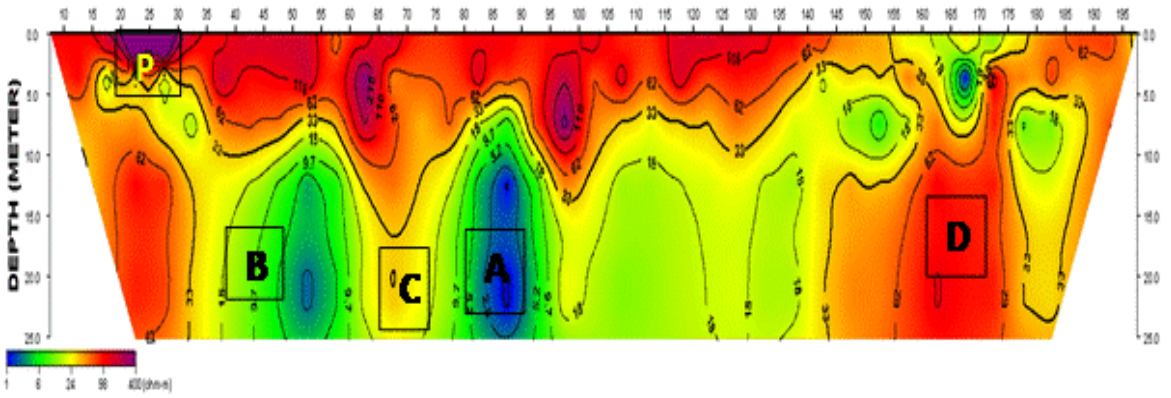

(a)

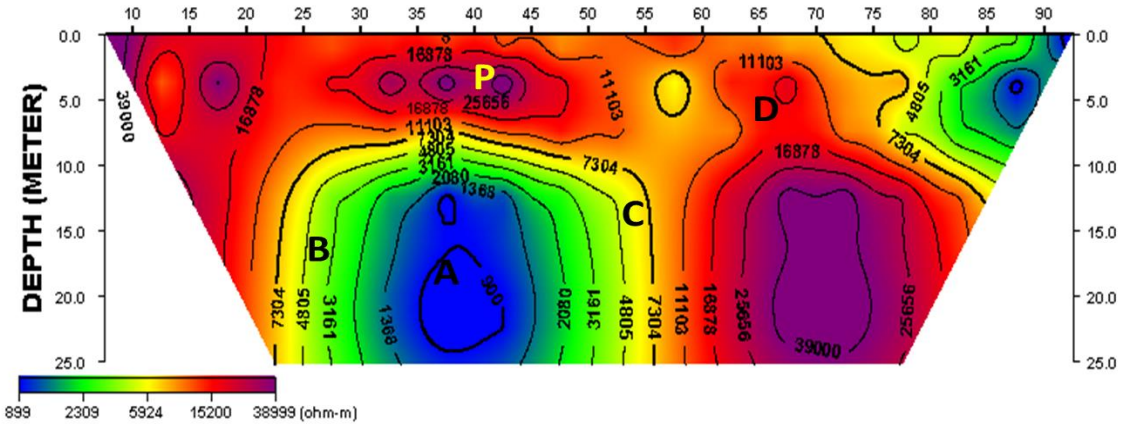

(b)

Article DOI: 10.52589/AJENSR-DDBGL2HW
DOI URL: https://doi.org/10.52589/AJENSR-DDBGL2HW

African Journal of Environment and Natural Science Research
ISSN: 2689-9434
Volume 6, Issue 3, 2023 (pp. 67-87)
www.abjournals.org

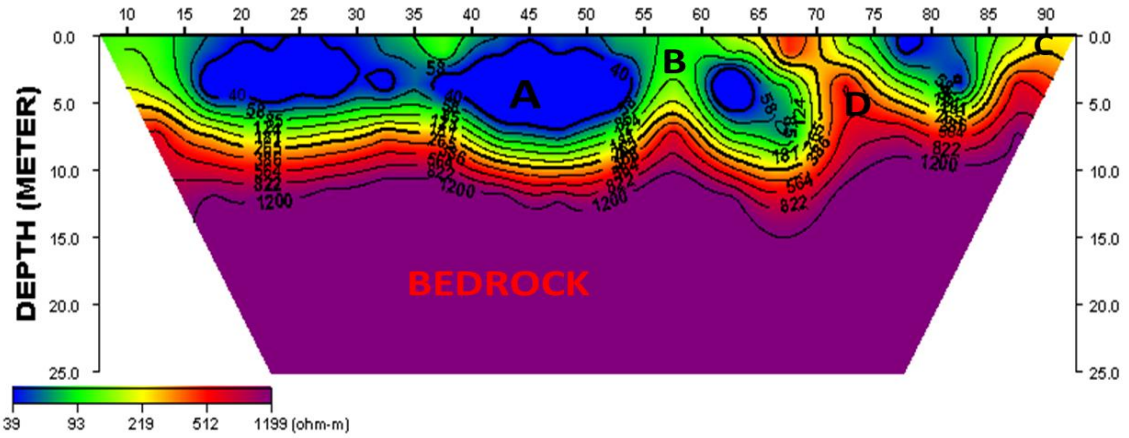

(c)

Figure 6: Pseudo-section of the dipole-dipole array for Awka Site 1

Profile 4

Profile 4 was laid 3 m west of the soil subsidence (Figure 7a). A profile length of 100m was surveyed with an electrode spacing of 5m. The depth probed was 25 m. The resistivity for this profile ranges from 149–110000 Ωm. At the top of the profile, between electrode 25 and 30 is the zone labeled P with an approximate resistivity of 80000 Ωm that is penetrating a depth of 3 m. The zone is considered to be filled with eroded structures. Sandwiching this high resistivity is a thin structure, labelled B, the clayey zone with resistivity of ~1000 Ωm. This zone acts like a blanket that prevents further erosion from occurring in the profile. Covering 60% of the profile is the bedrock with a very high resistivity that is more than 110000 Ωm.

Profile 5

Profile 5 was laid on the top of the soil subsidence (Figure 7b). The profile length surveyed is 100 m and a depth of 25 m was probed with an electrode spacing of 5 m. The range of resistivity for this profile is characterized from 149–330000 Ωm. The top of the profile shows regions with topsoil materials having a low resistivity of ~200 Ωm and reaching a depth of 2 m; these regions coincide with the soil subsidence at the top of the profile. A thin layer of clay soil, labeled B with resistivity of ~1000 Ωm, stretches beneath the topsoil from one end of the profile to the other end, preventing the penetration of topsoil materials and the formation of soil pipes in the subsurface. There are also stratified zones labeled C and D, which are sandy clay and fine sands, and are stretching thinly across the profile, just beneath the clayey soil.

Profile 6

Profile 6 was placed 3 meters east of the soil subsidence (Figure 7c) and surveyed to a length of 100 meters achieving probe depth of 25 meters with an electrode spacing of 5 meters. The measured resistivity of this profile varied from 49 to 499,999 Ωm across the surveyed area. Just like in Profile 4, the top of Profile 6 revealed patches of thick, clayey soil labeled as 'B', which had an approximate resistivity of 400 Ωm that prevents topsoil material penetration and tunnel erosion formation. On the surface of the profile, a zone of fine sand labeled as 'D', with an approximate resistivity of 20,000 Ωm, was detected between the electrode spacing of 25 and

Article DOI: 10.52589/AJENSR-DDBGL2HW
DOI URL: https://doi.org/10.52589/AJENSR-DDBGL2HW

African Journal of Environment and Natural Science Research
ISSN: 2689-9434
Volume 6, Issue 3, 2023 (pp. 67-87)
www.abjournals.org

30 meters, which coincides with the labeled 'P' portion of Profile 4. It can indicate that soil piping forms in these regions.

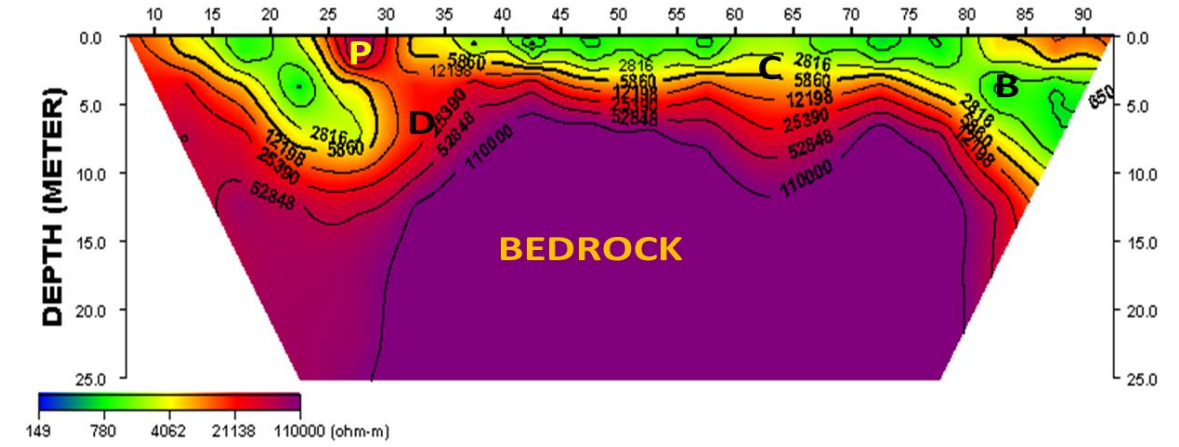

(a)

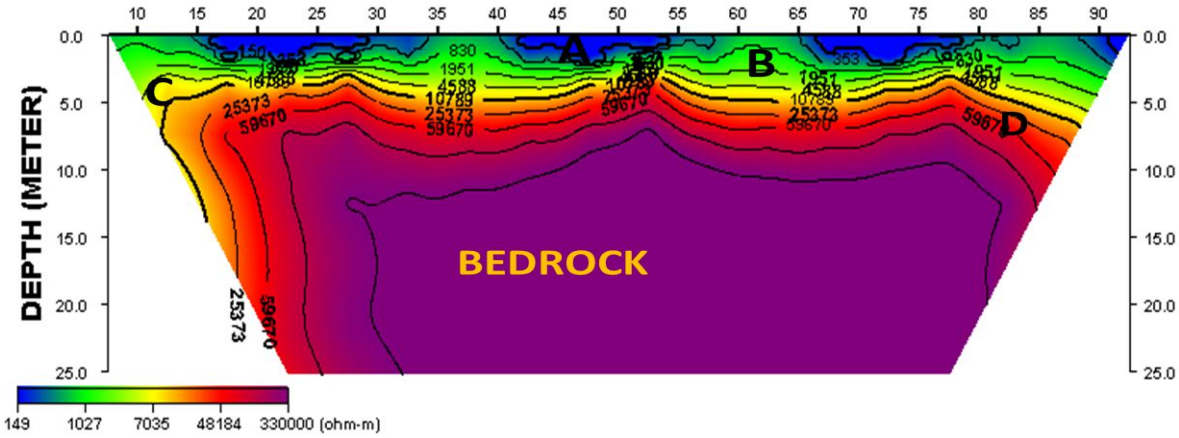

(b)

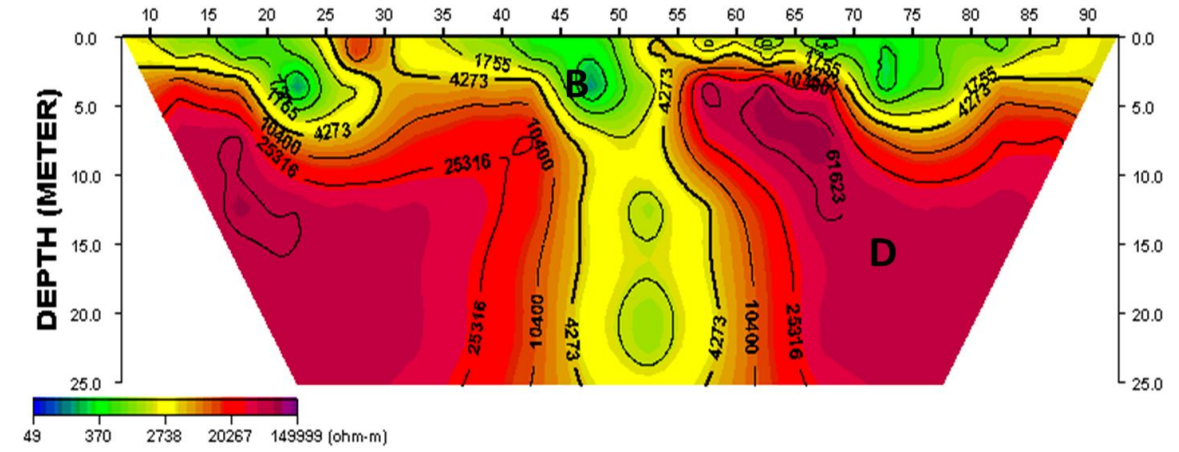

(c)

Figure 7: Pseudo-section of the dipole-dipole array for Awka Site 2

Article DOI: 10.52589/AJENSR-DDBGL2HW
DOI URL: https://doi.org/10.52589/AJENSR-DDBGL2HW

African Journal of Environment and Natural Science Research
ISSN: 2689-9434
Volume 6, Issue 3, 2023 (pp. 67-87)

www.abjournals.org

DISCUSSION

Soil pipes, which are void spaces beneath the Earth's surface resulting from extensive drainage by subsurface run-off water, serve as a convenient basis for comparison. These void spaces or drained soils are typically characterized by high resistivity, as documented in previous studies (Onwuegbuchulam et al., 2013; Osinowo & Olayinka, 2012). Consequently, the presence of these pipes in the subsurface causes a decrease in conductivity, resulting in a negative current density anomaly when applying the Fraser filtering technique, as well as a color range from dark blue to light blue when using the Karous-Hjelt filtering method. Hence, regions exhibiting negative current anomalies or displaying a dark blue coloration along the VLF-EM profiles are interpreted as soil pipes. For the ERT, these pipes are represented as high resistivity.

According to the VLF models, the soil pipes can be identified as low conductivity zones, ranging approximately from -10 to 0.5 Mhos. These zones extend vertically from 0m to 10m for both Profiles 1 and 3. Their horizontal dimensions span from 33 m to 37 m for Profile 1, and from 60 m to 65 m for Profile 3, approximately 5 m in each case. On the other hand, areas exhibiting moderate to high conductivity are interpreted as crystalline rocks, since such rocks lack drained soil and often contain saline pore spaces, as reported in previous research (Onwuegbuchulam et al., 2013). Consequently, the affected areas or regions where soil piping in the subsurface is likely to be prevalent are within Profiles 1 and 3, as depicted in Figure 5.

The dipole-dipole surveys was done on six profiles, which showcased the outcomes of 2D resistivity imaging obtained through an inversion method. This method involved nine iterations, resulting in a Root Mean Square (RMS) error of 7.4%. Given the anisotropic nature of the study areas, the subsurface was partitioned into six distinct structures, each with its characteristic resistivity range: saturated fault/fracture zones (10–3000 Ωm), clay (10–100 Ωm), sandy clay (100–3000 Ωm), sand (1000–10000 Ωm), eroded soil (3000–30000 Ωm), and bedrocks (3000 Ωm to ∞). These structures are depicted in Figure 6 and Figure 7.

Notably, the high resistivity structures (≥3000 Ωm), particularly those in close proximity to the surface of the profiles, are interpreted as eroded formations. These eroded structures possess a dispersive nature, which promotes the formation of soil piping. This dispersive behavior arises from the differentiation of soil resulting from the runoff of rainwater, as documented by Joshi et al. (2021) and Onda (1994).

CONCLUSION

Based on the findings of our study, it is evident that subsurface low conductivity zones, ranging from -10 to 0.5 Mhos, are present both within and surrounding the piping zones. This discovery strongly suggests the existence of subsurface cavities. The validity of this observation is further supported by the correlation between the negative amplitude responses of the Fraser filtering, the presence of thick blue patches (indicating low conductivity areas) in the Karous-Hjelt filtering model, and the identification of soil piping features in the study areas.

Furthermore, our data reveals that a significant portion (80%) of the pseudosection low conducting zones originates from the top of the profile, indicating a downward trend in the formation of piping. This information provides valuable insight into the behavior and characteristics of the piping phenomenon.

Article DOI: 10.52589/AJENSR-DDBGL2HW
DOI URL: https://doi.org/10.52589/AJENSR-DDBGL2HW

In addition, it can be inferred that subsurface voids in the study areas extend vertically downward up to 10 meters, with an average horizontal extension exceeding 0.5 meters. This emphasizes the substantial spatial reach of the subsurface voids, highlighting their potential impact on the surrounding environment.

The dipole-dipole survey conducted in the study area has provided insights into the structural anisotropic behavior, leading to the identification of six distinct structures. Among these structures, the eroded formation, characterized by a resistivity range of 1200–30000 Ωm, stands out as a significant contributor to the favorable conditions for soil piping. Additionally, the presence of strong dispersive soils further exacerbates the likelihood of soil piping occurrences within this particular structure. These findings shed light on the potential mechanisms underlying soil piping formation in the study area, underscoring the importance of considering the interplay between eroded formations, resistivity characteristics, and the presence of dispersive soils in understanding and managing soil piping phenomena.

Acknowledgement

We will like to acknowledge the staff of Anambra State Ministry of Works and Anambra Material Laboratory.

Author Contributions

The two authors contributed equally to the success of this work.

REFERENCES

Atallah, N., Shakoor, A., & Watts, C. F. (2015). Investigating the potential and mechanism of soil piping causing water-level drops in Mountain Lake, Giles County, Virginia. *Engineering Geology*, *195*, 282–291. https://doi.org/10.1016/j.enggeo.2015.06.001

Bernatek-Jakiel, A., & Kondracka, M. (2016). Combining geomorphological mapping and near surface geophysics (GPR and ERT) to study piping systems. *Geomorphology*, *274*, 193–209. https://doi.org/10.1016/j.geomorph.2016.09.018

Bernatek-Jakiel, A., & Poesen, J. (2018). Subsurface erosion by soil piping: Significance and research needs. *Earth-Science Reviews*, *185*, 1107–1128. https://doi.org/10.1016/j.earscirev.2018.08.006

Bernatek-Jakiel, A., & Wrońska-Wałach, D. (2018). Impact of piping on gully development in mid-altitude mountains under a temperate climate: A dendrogeomorphological approach. *CATENA*, *165*, 320–332. https://doi.org/10.1016/j.catena.2018.02.012

Carrazza, L., Moreira, C., & Portes, L. (2016). Gully cavity identification through electrical resistivity tomography. *Revista Brasileira de Geofísica*, *34*. https://doi.org/10.22564/rbgf.v34i2.799

Castañeda, C., Javier Gracia, F., Rodríguez-Ochoa, R., Zarroca, M., Roqué, C., Linares, R., & Desir, G. (2017). Origin and evolution of Sariñena Lake (central Ebro Basin): A piping-based model. *Geomorphology*, *290*, 164–183. https://doi.org/10.1016/j.geomorph.2017.04.013

Article DOI: 10.52589/AJENSR-DDBGL2HW
DOI URL: https://doi.org/10.52589/AJENSR-DDBGL2HW

Chibuogwu, I. U., & Ugwu, G. Z. (2023a). An Open Investigation of Some Soil Pipes Forming Soil Subsidence at Awka South Local Government Area Using Very Low Frequency Electromagnetic Geophysical Technique. *International Journal of Scientific Research in Multidisciplinary Studies*, *9*(2), 40–45.

Chibuogwu, I. U., & Ugwu, G. Z. (2023b). Chemical Analysis of Uncontrolled Soil Pipes Leading to Soil Subsidence in Anambra State Nigeria. *International Journal of Scientific Research in Multidisciplinary Studies*, *9*(1), 40–45.

Chibuogwu, I. U., & Ugwu, G. Z. (2023c). Uncovering soil piping vulnerability using direct current geophysical techniques in Awka, Anambra State, Nigeria. *International Journal of Multidisciplinary Research and Growth Evaluation*, *4*(3), 426–450. https://doi.org/10.54660/.IJMRGE.2023.4.3.426-450

Dodds, J. (2003). PARTICLE SHAPE AND STIFFNESS - EFFECTS ON SOIL BEHAVIOR -Thesis Presented to The Academic Faculty. *Geogia Institute of Technology*.

Ezenkwen, E. (2010). Gully Erosion in Anambra State: Nnaka. *Patrotic Union Journal*, *1*, 9–18.

Fraser, D. C. (1996). Contouring of VLF-EM Data. *Geophysics*, *54*, 245–253.

García-Ruiz, JoséM., Lasanta, T., & Alberto, F. (1997). Soil erosion by piping in irrigated fields. *Geomorphology*, *20*(3–4), 269–278. https://doi.org/10.1016/S0169-555X(97)00028-7

Graham, C. B., & Lin, H. (2012). Chapter 18 - Subsurface Flow Networks at the Hillslope Scale: Detection and Modeling. In H. Lin (Ed.), *Hydropedology* (pp. 559–593). Academic Press. https://doi.org/10.1016/B978-0-12-386941-8.00018-6

J. O. Coker, H. H. Akpan, A. O. Atilade, & O. F. Ojo. (2020). Seasonal Comparison of Potential Groundwater Aquifer in Ijebu-Ife, South-West, Nigeria, using Dipole-Dipole Array and Electromagnetic Methods. *Journal of the Nigerian Society of Physical Sciences*, 241–249. https://doi.org/10.46481/jnsps.2020.128

Jones, J. A. A., Richardson, J. M., & Jacob, H. J. (1997). Factors controlling the distribution of piping in Britain: A reconnaissance. *Geomorphology*, *20*(3–4), 289–306. https://doi.org/10.1016/S0169-555X(97)00030-5

Joshi, M., Prasobh, P. R., Rajappan, S., Rao, B. P., Gond, A., Misra, A., Eldhose, K., Nandakumar, V., & Tomson, J. K. (2021). Detection of soil pipes through remote sensing and electrical resistivity method: Insight from southern Western Ghats, India. *Quaternary International*, *575–576*, 51–61. https://doi.org/10.1016/j.quaint.2020.08.021

Kaikkonen, P., & Sharma, S. P. (1998). 2-D nonlinear joint inversion of VLF and VLF-R data using simulated annealing. *Journal of Applied Geophysics*, *39*(3), 155–176. https://doi.org/10.1016/S0926-9851(98)00025-1

Karous, M., & Hjelt, S. E. (1983). LINEAR FILTERING OF VLF DIP-ANGLE MEASUREMENTS*. *Geophysical Prospecting*, *31*(5), 782–794. https://doi.org/10.1111/j.1365-2478.1983.tb01085.x

Li, Z.-X., & Rao, S.-W. (2019). The determination of frequency domain soil parameters of horizontally layered structure by using dipole-dipole array. *International Journal of Numerical Modelling: Electronic Networks, Devices and Fields*, *32*(5), e2578. https://doi.org/10.1002/jnm.2578

Loke, M. H., & Barker, R. D. (1996). Rapid least-squares inversion of apparent resistivity pseudosections by a quasi-Newton method1. *Geophysical Prospecting*, *44*(1), 131–152. https://doi.org/10.1111/j.1365-2478.1996.tb00142.x

Article DOI: 10.52589/AJENSR-DDBGL2HW
DOI URL: https://doi.org/10.52589/AJENSR-DDBGL2HW

Monteiro Santos, F. A., Mateus, A., Figueiras, J., & Gonçalves, M. A. (2006). Mapping groundwater contamination around a landfill facility using the VLF-EM method—A case study. *Journal of Applied Geophysics*, *60*(2), 115–125. https://doi.org/10.1016/j.jappgeo.2006.01.002

Neyamadpour, A., Wan Abdullah, W. A. T., Taib, S., & Neyamadpour, B. (2010). Comparison of Wenner and dipole–dipole arrays in the study of an underground three-dimensional cavity. *Journal of Geophysics and Engineering*, *7*(1), 30–40. https://doi.org/10.1088/1742-2132/7/1/003

Nich, O., & Okeke-Ogbu, C. J. (2017). Erosion Problems and their impact in Anambra State, Nigeria (A case study of Nnaka Community). *International Journal of Environment and Pollution Research*, *5*, 24–87.

Ogilvy, R. D., & Lee, A. C. (1991). INTERPRETATION OF VLF-EM IN-PHASE DATA USING CURRENT DENSITY PSEUDOSECTIONS1. *Geophysical Prospecting*, *39*(4), 567–580. https://doi.org/10.1111/j.1365-2478.1991.tb00328.x

Onda, Y. (1994). Seepage erosion and its implication to the formation of amphitheatre valley heads: A case study at Obara, Japan. *Earth Surface Processes and Landforms*, *19*(7), 627–640. https://doi.org/10.1002/esp.3290190704

Onwuegbuchulam, D. O., Ikoro, D. O., Nwugha, V. N., & Okereke C. N. (2013). Application of Very Low Frequency-Electromagnetic (VLF-EM) Method to Map Fractures/Conductive Zones in Auchi South western Nigeria. *The International Journal Of Engineering And Science (IJES)*, *5*(5), 07–13.

Osinowo, O. O., & Olayinka, A. I. (2012). Very low frequency electromagnetic (VLF-EM) and electrical resistivity (ER) investigation for groundwater potential evaluation in a complex geological terrain around the Ijebu-Ode transition zone, southwestern Nigeria. *Journal of Geophysics and Engineering*, *9*(4), 374–396. https://doi.org/10.1088/1742-2132/9/4/374

Palacky, G. J. (1981). THE AIRBORNE ELECTROMAGNETIC METHOD AS A TOOL OF GEOLOGICAL MAPPING*. *Geophysical Prospecting*, *29*(1), 60–88. https://doi.org/10.1111/j.1365-2478.1981.tb01011.x

Palacky, G. J., Ritsema, I. L., & Jong, S. J. (1981). ELECTROMAGNETIC PROSPECTING FOR GROUNDWATER IN PRECAMBRIAN TERRAINS IN THE REPUBLIC OF UPPER VOLTA*. *Geophysical Prospecting*, *29*(6), 932–955. https://doi.org/10.1111/j.1365-2478.1981.tb01036.x

Parker, G. G., Higgins, C. G., Parker, G. G., & Wood, W. W. (1990). Chapter 4. Piping and pseudokarst in drylands. In *Geological Society of America Special Papers* (Vol. 252, pp. 77–110). Geological Society of America. https://doi.org/10.1130/SPE252-p77

Patti, G., Grassi, S., Morreale, G., Corrao, M., & Imposa, S. (2021). Geophysical surveys integrated with rainfall data analysis for the study of soil piping phenomena occurred in a densely urbanized area in eastern Sicily. *Natural Hazards*, *108*(3), 2467–2492. https://doi.org/10.1007/s11069-021-04784-9

Sidle, R. C., Kitahara, H., Terajima, T., & Nakai, Y. (1995). Experimental studies on the effects of pipeflow on throughflow partitioning. *Journal of Hydrology*, *165*(1), 207–219. https://doi.org/10.1016/0022-1694(94)02563-Q

Uchegbu, J. N. (2004). The role of Government and Citizens in Erosion Control, in H.C Mbah et al: Management of Environmental Problems and Hazard in Nigeria. *Ashgate Publishing LTD Cower House. Croft Road Aldrshot Gill 3HR England.*

Article DOI: 10.52589/AJENSR-DDBGL2HW
DOI URL: https://doi.org/10.52589/AJENSR-DDBGL2HW

Vannoppen, W., Verachtert, E., & Poesen, J. (2017). Pipeflow response in loess-derived soils to precipitation and groundwater table fluctuations in a temperate humid climate: Pipeflow response to precipitation and groundwater table fluctuations. *Hydrological Processes*, *31*(3), 586–596. https://doi.org/10.1002/hyp.11049

Wilson, G. V., Cullum, R. F., & Römkens, M. J. M. (2008). Ephemeral gully erosion by preferential flow through a discontinuous soil-pipe. *CATENA*, *73*(1), 98–106. https://doi.org/10.1016/j.catena.2007.09.008

Zhang, T., & Wilson, G. V. (2013). Spatial distribution of pipe collapses in Goodwin Creek Watershed, Mississippi: SPATIAL DISTRIBUTION OF PIPE COLLAPSES. *Hydrological Processes*, *27*(14), 2032–2040. https://doi.org/10.1002/hyp.9357

Zhu, T. X., Luk, S. H., & Cai, Q. G. (2002). Tunnel erosion and sediment production in the hilly loess region, North China. *Journal of Hydrology*, *257*(1), 78–90. https://doi.org/10.1016/S0022-1694(01)00544-3

Zohdy A.A.R. (1965). The Auxilliary Point Method of Electrical sounding Interpretation and its Relationship to Dar Zorrouk Parameters. *Geophysics*. 30: 644-650.

Zohdy AAR, Eaton GP and Mabey DR. (1974). Application of Surface Geophysics to Groundwater Investigations. Techniques of Water Resources Investigations of U.S. Geol. Survey: Book 2, Chapter DI. U.S. Government Printing Office: Washington, D.C., USA. p. 66.

Koefoed O. (1979). Geosounding Principles, 1. Resistivity Sounding Measurements. *Elsevier Scientific Publishing*: Amsterdam, Netherlands. p. 275.

Keller G.V. and Frishchncht F.C. (1966). Electrical Methods in Geophysical Prospecting. Pergamon Press: New York, NY. p. 96.

Vander Velpen, B.P.A. (2004). WinRESIST Version 1.0. Resistivity Sounding Interpretation Software. M.Sc. Research Project, ITC, Delft Netherland.

Environment and Social Management Plan. Introduction to Environment Basic Concept.Teaching conducting agency. pp.21-26, 2016.

Article DOI: 10.52589/AJENSR-DDBGL2HW
DOI URL: https://doi.org/10.52589/AJENSR-DDBGL2HW